Dynamic modeling of district heating network based on discrete event simulation

Zichan Xie

Aalto University

Aalto University publication series
Doctoral Theses 75/2025

Dynamic Modeling of District Heating Network Based on Discrete Event Simulation

Zichan Xie

A doctoral thesis completed for the degree of Doctor of Science (Technology) to be defended, with the permission of the Aalto University School of Science, at a public examination held at the H304 (Otakaari 1, Espoo, Finland) of the school on 16 May 2025 at 12 noon.

Aalto University
School of Science
Department of Mathematics and System Analysis

Supervising professor
Professor Risto Lahdelma, Aalto University, Finland

Thesis advisors
Academy Research Fellow Haichao Wang, Aalto University, Finland

Preliminary examiners
Associate Professor Rongling Li, Technical University of Denmark, Denmark
Professor Henrik Saxén, Åbo Akademi University, Finland

Opponent
Professor Henrik Saxén, Åbo Akademi University, Finland

Aalto University publication series
Doctoral Theses 75/2025

© Zichan Xie

ISBN 978-952-64-2487-3 (paperback)
ISBN 978-952-64-2488-0 (pdf)
ISSN 1799-4934 (print)
ISSN 1799-4942 (pdf)

https://urn.fi/URN:ISBN:978-952-64-2488-0

Unigrafia Oy
Helsinki 2025

Finland

Aalto-yliopisto

ABSTRACT

Author Zichan Xie

Name of the doctoral thesis Dynamic Modeling of District Heating Network Based on Discrete Event Simulation

Article-based thesis

Number of pages 97

Keywords Discrete event simulation; Lagrangian method; Variable time step; Dynamic hydraulic-thermal simulation; District heating network

Heating and cooling play important roles in saving energy and reducing emissions. Despite the potential of district heating (DH) systems to apply sustainable energy sources efficiently, DH accounts for only 8% of global heat consumption. The evolution of intelligent DH systems is constrained by insufficient digitalization, metering, and monitoring, which hinder effective optimization and planning. Addressing these challenges inevitably requires advanced dynamic simulation models that balance computational speed, accuracy, and adaptability for complex DH networks.

This research develops a flexible, accurate, and efficient dynamic DH network model based on the Lagrangian method. The model employs variable time step simulation within a discrete event simulation (DES) framework, offering key operational insights such as delivered temperature and energy, water transmission time, and heat losses. It can simulate complex meshed network topologies and diverse operational strategies, including "variable flow, variable temperature", making it suitable for real-world applications.

Real-world validations, including tests on a single pipe, a tree-shaped network, and a meshed network, verify the model's high performance. For instance, an 85-day simulation of a meshed network with 186 pipes was completed in 0.29 seconds on a laptop (Intel Core i7-1185G7 CPU @ 3.00 GHz), achieving a mean residual standard deviation of 1.15 °C across 80 substations. These results highlight the DES model's potential for integration into future holistic system studies, empowering operators to optimize performance and advance the transition toward more sustainable and efficient heating systems.

The study establishes a robust foundation for variable time step simulation through critical sampling point identification and adaptive local updates based on lazy evaluation principles. The developed model dynamically adjusts temporal and spatial discretization to ensure accuracy, reducing computation time and minimizing numerical errors by avoiding unnecessary intermediate calculations. Additionally, a technique, called the tolerance threshold, by eliminating redundant sampling points improves computational efficiency without significantly compromising accuracy.

This work not only provides a versatile tool for dynamic modeling of DH networks but also demonstrates the broader potential of variable time step simulations using the DES framework. By addressing key challenges in the development of the high-performance dynamic model, it will encourage the adoption of similar techniques across other energy system components.

Preface

Pursuing a PhD has been my dream since childhood. However, throughout the doctoral journey, I have come to deeply understand the gap between aspirations and reality. Reflecting on the past four years, I would describe this experience as a continuous cycle of falling and finding the courage to stand back up. Along the way, I have wrestled with self-doubt, anxiety about uncertain outcomes, and fear of new challenges. Yet, these struggles were accompanied by moments of accomplishment, excitement in problem-solving, and the satisfaction of exploring uncharted territory.

This journey has been a catalyst for my growth—not only in developing my professional skills and broadening my perspective but also in shaping my character. It has made me more resilient, given me the courage to confront challenges, and taught me to embrace failure. These lessons will undoubtedly help me face the inevitable ups and downs of life with composure and confidence.

Reaching this milestone would not have been possible without my own persistence and the unwavering support of those around me. I am deeply grateful to everyone who encouraged me during difficult times and believed in my potential.

First and foremost, I would like to thank my supervisor, Professor Risto Lahdelma. Four years ago, he gave me the opportunity to come to Finland to pursue a PhD. Since then, he has provided consistent and patient guidance, generously shared his knowledge, fully trusted me, and never hesitated to offer praise and encouragement. His rigorous approach to research and his enthusiasm in discovering and solving problem have deeply inspired me. As a young researcher just starting out, I feel incredibly fortunate to have a such supportive supervisor.

I also want to thank my advisor, Professor Haichao Wang, for providing funding and valuable direction for my research. I would like to thank my co-authors, Pengmin and Maximilian; their insights have been invaluable to my papers.

I want to express my heartfelt thanks to my office colleagues, Joaquin, Piyalee, Helmi, Leevi, and everybody else at Systems Analysis Laboratory. The coffee breaks and teatimes we shared were a welcome escape from long hours of work and reminded me that there is more to life than just work. A special thanks goes to my buddy, Olli, who warmly welcomed me and helped me integrate into this new environment when I first arrived in Finland. My colleagues' kindness and mutual support created a relaxed and enjoyable workplace atmosphere. It felt like being part of a large family made up of people from all over the world, and I am honored to have had the chance to work alongside them.

I would also like to thank Professor Fabricio Oliveira. Although he was not directly involved in supervising my work, he was always friendly and willing to offer help during our conversations, which I greatly appreciate.

I would also like to thank my family and friends. Without my parents' support, I would not have had the chance to follow my dream. My friends have been a pillar of support throughout this journey, always ready to listen and offer encouragement, even across different countries and time zones. To my friends who are also pursuing a PhD, I would like to say: I deeply appreciate your understanding and shared experiences.

Finally, many thanks go to my boyfriend Petar and my cat Pichu. They have been my constant source of joy and comfort, helping me unwind after long days of work. While my boyfriend may not be fascinated about the details of my research, he has patiently listened to my challenges and continuously encouraged me. He has always believed in my ability to succeed, yet he has also reassured me that it is okay to pause if I ever feel overwhelmed. For someone like me, raised in a high-pressure competitive environment, those words mean more than I can express. Thank you for your understanding, patience, and unchanged companionship throughout this journey.

Espoo, March 24, 2025

Zichan Xie

Contents

List of Publications

This doctoral thesis is based on the following publications which are referred to in the text by their Roman numerals.

I. Xie Zichan, Wang Haichao, Hua Pengmin, Lahdelma Risto. Discrete event simulation for dynamic thermal modelling of district heating pipe. *Energy* 2023;285:129523. https://doi.org/10.1016/j.energy.2023.129523

II. Xie Zichan, Wang Haichao, Hua Pengmin, Björkstam Maximilian, Lahdelma Risto. Dynamic thermal simulation of a tree-shaped district heating network based on discrete event simulation. *Energy* 2024;313:133775. https://doi.org/10.1016/j.energy.2024.133775.

III. Xie Zichan, Wang Haichao, Hua Pengmin, Lahdelma Risto. Hydraulic-thermal dynamic model of meshed district heating network based on discrete event simulation. Under review in *Energy Conversion and Management*.

Author's Contribution

Publication I: Discrete event simulation for dynamic thermal modelling of district heating pipe

Xie is the primary author. She drafted the manuscript, handling tasks including curating the data, conducting the investigation, validating the model, and visualizing results. Lahdelma proposed the idea, supervised this work, and collaborated with Xie to conceptualize the methodology and develop the model. Wang provided funding and led this project. All authors worked together on reviewing and improving the manuscript.

Publication II: Dynamic thermal simulation of a tree-shaped district heating network based on discrete event simulation

Xie is the primary author, developing the model and drafting the manuscript. She curated the data, conducted the investigation, validated the model, and visualized and analyzed the results. Lahdelma supervised the work and participated in model development. Wang secured funding and managed the project. Björkstam provided the measurement data and contributed to the investigation. All authors collaborated on reviewing and improving the manuscript.

Publication III: Hydraulic-thermal dynamic model of meshed district heating network based on discrete event simulation

Xie is the primary author. She drafted the manuscript and developed the model, handling tasks such as curating the data, conducting the investigation, validating the model, and visualizing and analyzing the results. Lahdelma supervised the work and helped with model development. Wang is the project manager, providing funding and data. All authors cooperated in reviewing and improving the manuscript.

List of Abbreviations

CFL	Courant–Friedrichs–Lewy criterion
DES	Discrete event simulation
DH	District heating
DHC	District heating and cooling
Deque	Double-ended queue
FEM	Finite element method
FDM	Finite difference method
FVM	Finite volume method
ME	Mean error
RSD	Residual standard deviation
VFVT	“Variable flow, variable temperature” operational strategy
4GDH	4^{th} generation of district heating systems
5GDH	5^{th} generation of district heating systems

List of Symbols

A	Cross-section area of pipe, m²
c_p	Specific heat capacity of water, J/(kg·K)
D	Half-distance between the centers of the hot and cold pipes, m
D_w	Diameter of cross-section area (= inner diameter of the pipe wall), m
F_{Next}	The next arriving water frontier
f	Friction factor
H	Buried depth from the pipe center to the ground surface, m
L	Pipe length, m
m	Mass flow rate, kg/s
p	Pressure potential, Pa
Re	Reynold's number
r_i	Inner radii of the insulation layer (= outer radii of the pipe wall), m
r_o	Outer radii of the insulation layer of pipe, m
T_c	Water temperature of cold pipe, °C
T_h	Water temperature of hot pipe, °C
T_g	Ground temperature, °C
T_{in}	Water temperature of a water frontier when it is created, °C
T_{out}	Water temperature of a water frontier when it arrives at the outlet, °C
t	Simulation time, s
t_{in}	Creation time of a water frontier, s
t_{out}	Arrival time of a water frontier, s
v	Flow velocity, m/s
ρ	Density of water, kg/m³

ε	Absolute roughness of pipe wall, m
τ	Travel time of water particle or frontier, s
λ_g	Heat conductivity of soil, W/(m·K)
λ_i	Heat conductivity of insulation, W/(m·K)
Δt	Time step, s
Δx	Space step, m

1 Introduction

1.1 Background

Energy for heating and cooling accounts for nearly 50% of the EU's total gross final energy consumption, with three quarters of this demand still being met by fossil fuels. Despite the potential of district heating and cooling (DHC) systems to efficiently apply sustainable energy sources for heating and cooling (Moreno et al., 2024), district heating (DH) represents only about 8% of total final heat consumption worldwide (European Commission. Directorate General for Energy., 2024).

A report by the European Commission (2022) highlights the barriers to achieving the long-term goal of a carbon-neutral energy supply by 2050. One technological challenge for developing efficient and renewable district heating (DH) systems is the insufficient digitalization, metering, and monitoring of DH networks. This lack of insight into operational parameters limits the operator's ability to effectively control the DH system and meet actual demand.

Completely rebuilding a new system is expensive and impractical. Therefore, improving the efficiency of DH systems must consider the existing infrastructure and conditions. Among innovative DHC approaches, fourth-generation district heating (4GDH) systems are particularly suitable for such upgrades (Calise et al., 2023; Gudmundsson et al., 2022; Volkova et al., 2022). These systems emphasize precise and efficient energy delivery, relying heavily on intelligent control and holistic system optimization (Lund et al., 2014).

Conducting effective operational studies is essential for enhancing system performance by enabling real-time analysis and decision-making that align with actual demand. Comprehensive planning and optimization of DH systems require continuous monitoring of temperature changes within DH networks. This monitoring is important for the successful implementation of closed-loop control (Bergsteinsson et al., 2022). Dynamic network simulation offers an economical approach to obtain the necessary temperature feedback (Betancourt Schwarz et al., 2019; Sartor & Dewalef, 2017). Nonetheless, one significant limitation of these large-scale dynamic network simulations is the considerable computational time they require (Brown et al., 2022).

1.2 State-of-the-art

This study focuses on physical models grounded in well-established principles of fluid dynamics and thermodynamics, rather than data-driven models, due to two significant limitations of the latter in broader applications. First, data-driven models require extensive, high-quality measurement data for training. However, many DH networks lack advanced devices, and existing sensors are often outdated, uncalibrated, or poorly maintained. Historical data is either unavailable or limited in scope, making machine learning models impractical for many projects. These data deficiencies also restrict their effectiveness in tasks like fault detection, which require consistent and accurate records. Second, machine learning models are tailored to current network configurations and operational strategies. As a result, they are unable to simulate future scenarios, such as network upgrades or structural modifications, which are essential for research aimed at improving DH networks.

In fluid mechanics, two primary methods are used to describe the motion of fluid particles: the Eulerian approach and the Lagrangian approach. In the Eulerian method, the fluid flow is analyzed at fixed locations in space, focusing on the properties such as velocity, pressure, and density over time, without tracking individual particles. Conversely, the Lagrangian approach follows individual fluid particles as they move through space and time, tracking their properties and providing a detailed understanding of their trajectories and interactions within the flow.

In computational fluid dynamics, most common commercial software, such as ANSYS, relies on the Eulerian method. This approach integrates seamlessly with grid-based techniques, including finite difference method (FDM), finite volume method (FVM), and finite element method (FEM), making it robust and efficient for solving complex three-dimensional problems. Additionally, it avoids the challenges of tracking a massive number of particles and grid distortion. This also made it a popular choice in many DH network models, as seen in widely used energy system modeling platforms like IDA ICE, Modelica, and TRNSYS. However, in DH network simulations, assuming *plug flow,* where a uniform velocity is assumed across all cross-sections of the heating pipes, reduces the problem to a one-dimensional system. In this context, the Lagrangian method may offer greater efficiency and accuracy (Price, 2006; Steinegger et al., 2023).

A review of existing DH network models based on the Eulerian approach highlights four challenges that hinder their efficiency in accurately simulating thermal dynamics:

1) <u>Dependence on fine spatial grids</u>: Regardless of whether FDM, finite FVM, or FEM is used, the accuracy of the simulation relies heavily on the refinement of the spatial grid. Coarse grids can cause numerical dissipation and inaccuracies, particularly in systems with sharp gradients. While finer

grids improve accuracy, they significantly increase computational costs due to the higher number of control volumes or elements.

2) Courant criterion and time step constraints in explicit methods: In explicit methods, where next state is determined by current or previous stage, the Courant–Friedrichs–Lewy (CFL) criterion must be satisfied to ensure numerical stability (Blazek, 2005). This criterion ($v\Delta t/\Delta x < \mathrm{CFL\ number}$) requires the time step Δt to be small enough that information does not propagate more than one spatial grid cell Δx during each step. This requires smaller time steps Δt as spatial steps Δx are reduced for higher accuracy. In DH networks, where flow velocities vary significantly between pipe segments (0.2 – 4 m/s (Guelpa, 2020)), a uniform time step must be extremely small to maintain accuracy in high-flow segments. This increases computational costs and may lead to instability if the criterion is not met.
3) Computational burden with implicit methods: Models based on implicit methods, where the future state is involved at the current step, bypass the CFL constraint and allow larger time steps. However, they require solving equation systems iteratively at each time step, which can be computationally expensive, especially for large and complex DH networks.
4) Trade-offs between accuracy and simulation time: Reducing the spatial and temporal step sizes improves model accuracy but increases simulation time. Additionally, the marginal improvements in accuracy decrease as step sizes become smaller, leading to inefficient use of computational resources. Identifying the optimal step sizes often requires multiple trial simulations, adding complexity and effort. Moreover, this strategy is hard to apply to network planning phase since there is no standard rule for step settings.

These challenges limit the efficiency and adaptability of Eulerian-based models for DH networks, especially in scenarios requiring accurate thermal simulations or flexible modeling. In contrast, the Lagrangian method allows variable spatial step sizes that adapt dynamically to time steps and flow speeds. This flexibility makes it a promising alternative for more efficient and accurate DH network simulations.

Lagrangian approach has been successfully implemented with FVM and applied to DH network simulation. In this method, the water temperature is assumed to be fully mixed within each control volume, with the control volume sizes dynamically generated during the simulation. The most well-known implementation of this approach is referred to as the "node method" (Benonysson, 1991). This method has been extensively validated and integrated into the commercial software EcoStruxure District Energy (formerly TERMIS), owned by Schneider Electric. It has been applied to many DH networks with advanced monitoring system. Similar implementations can be found in MATLAB (Dénarié et al., 2023), Python (Boghetti & Kämpf, 2024), TRNSYS (Sartor & Dewalef, 2017), and Modelica (Schweiger et al., 2017).

Lagrangian FVM models offer significant advantages over Eulerian-based approaches in terms of flexibility and accuracy, primarily due to their adaptable spatial discretization. However, these models can suffer from numerical inaccuracies stemming from the assumption of fully mixed temperatures. To address this issue, the Lagrangian method has been extended to simulate pipes using infinitesimal segments. Such implementations are primarily available in the Modelica environment, as seen in the IBPSA Modelica Library (van der Heijde, Fuchs, et al., 2017) and the DistrictHeating Modelica library (Giraud et al., 2015). These models adopt the spatialDistribution operator, which facilitates sampling, linear interpolation, and shifting stored data distributions, enabling tracking of time and temperature during simulations. Numerical studies indicate that these models achieve higher accuracy compared to Lagrangian FVM with coarse time steps, demonstrating potential for enhancing the efficiency of accurate DH network simulations. Nevertheless, the use of a universal built-in operator may present efficiency challenges (Falay et al., 2020).

1.3 Research gap

Numerous studies highlight the advantages of Lagrangian models over Eulerian models, particularly in terms of accuracy and computational efficiency. Among these, the infinitesimal segment method has emerged as a promising approach, capable of delivering accurate simulations even with coarser time steps. However, concerns about potential numerical instability have led some researchers to prefer FVM over the infinitesimal segment method (Schweiger et al., 2017).

Although employing variable time step simulation is meaningful for network modeling (Wu et al., 2025), all existing Lagrangian models currently rely on fixed time step simulations, where time steps are often set much smaller than the measurement intervals to ensure accuracy. While some models can achieve rapid simulations—completing 24-hour simulations of networks with 485 pipe segments in just 4 seconds (Dénarié et al., 2023)—this speed is still insufficient for large-scale system optimizations, which require iterative recalculations. Variable time step methods offer the potential to significantly enhance simulation efficiency by focusing updates only at critical sampling points while maintaining comparable accuracy. However, the absence of a theoretical framework to identify these critical points or prioritize significant temperature changes has limited their practical adoption.

The infinitesimal segment method is well-suited for simulating temperature propagation with variable time steps. Despite its potential, its application in DH systems has been overlooked, missing opportunities to develop faster and more accurate dynamic simulation methods (Klemm et al., 2023). Addressing this gap requires the establishment of a robust theoretical foundation for accurate and stable variable time step implementations. Additionally, identifying efficient methodologies to execute these simulations is challenging. Overcoming these obstacles is essential for unlocking the full potential of the infinitesimal segment method in dynamic DH system simulations.

Another gap in dynamic DH network modeling is considering heat transfer between parallel pipes. Its impact on heat losses is widely recognized (van der Heijde, Aertgeerts, et al., 2017), but only a few studies include it in network simulations (Dahm, 2001; H. Wang et al., 2018). The existing models that do address this issue are based on Eulerian FVM approaches, leaving a gap for Lagrangian models.

There is a clear need to develop new Lagrangian-based models that can handle variable time steps and consider heat transfer between parallel pipes.

1.4 Objective of the research

To address the computational efficiency bottleneck in existing models, this research aims to develop a dynamic, fast, accurate, and scalable tool capable of handling the complex iterative calculations required for holistic analysis and optimization of DH systems. To support effective system monitoring and control under various operational conditions, the proposed model is designed to provide the following operational insights into the network:

- The delivered water temperature at each customer or substation.
- The amount of heat energy each customer or substation can receive.
- The water transmission time from the heating plant to each customer or substation.
- The heat losses incurred during water transmission.

To achieve the functionalities outlined above, we put forth a Lagrangian model with variable time steps using Discrete Event Simulation (DES) framework. Within this context, we asked the following six research questions:

1) How can sampling points be strategically selected and dynamically updated within the variable time step framework to ensure computational efficiency and accuracy?
2) How can temperature changes in parallel pipes, such as twin pipes, be accurately calculated within a meshless modeling approach?
3) How can the variable time step simulation be implemented within the DES framework to optimize computational performance while preserving model fidelity?
4) How accurately does the developed model capture the thermal and hydraulic dynamics of the DH network?
5) How fast is the proposed model, and is it capable of supporting iterative calculations for large-scale network optimization?

6) What techniques can be applied to further improve the computational speed of the model without compromising accuracy?

The work progressively extends the DES model from pipe-level simulations to tree-shaped networks and finally to meshed networks. The six research questions are answered by targeting different network complexities, as summarized in Table 1.

Figure 1 presents the key differences and connections among the three studies, illustrating how each publication builds upon the previous one to advance the research. The detailed contribution of each paper can be found in Section 4, Research contributions.

Table 1 Answered research questions in publications I–III.

Publications	Network topologies	Answered research questions					
		1	2	3	4	5	6
I	Single pipe	X			X		
II	Tree-shaped network	X	X	X	X	X	X
III	Meshed network	X			X	X	

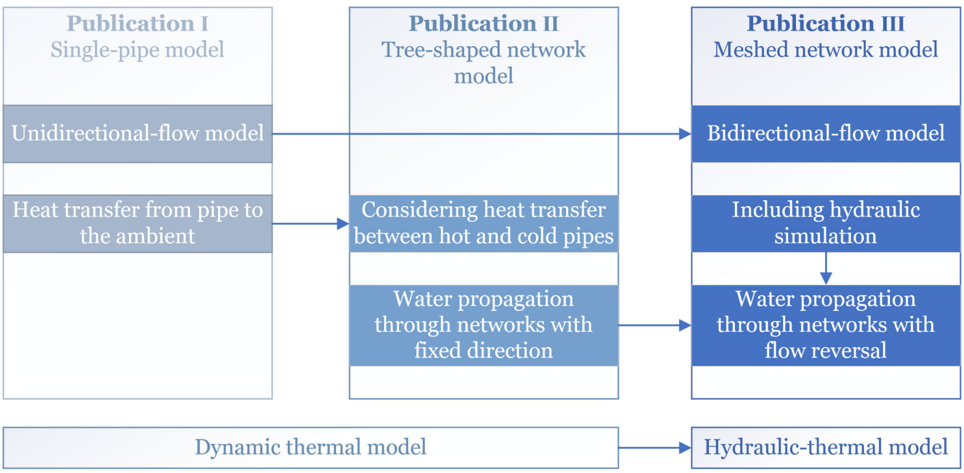

Figure 1 Development of DES model.

The ultimate purpose is to integrate these validated models into an online operational optimization tool, empowering operators to optimize performance and advance the transition toward more sustainable and efficient heating systems.

Unlike traditional fixed time step methods, the proposed DES framework adapts to system demands, improving computational efficiency and accuracy by applying variable time step modeling to DH networks. This research highlights the advantages of adaptive simulations for complex systems, where different components require variable time step resolutions to ensure both accuracy and efficiency. This innovation not only addresses challenges in DH modeling but also offers a practical example for adopting variable time step technique. With minor adjustments, this model could also be applied to district cooling networks. As energy systems become more complex, this demonstrated success of DES-based DH network simulation is expected to inspire applications of variable time step simulation across various components.

2 Methodology

The DES model is based on the following assumptions:

1) The model assumes plug-flow, meaning a uniform velocity profile across all cross-sections of the heating pipes. This assumption eliminates mixing and thermal diffusion in the axial direction, preserving sharp temperature fronts as the water moves through the network. This is appropriate for turbulent forced flow where convective heat transfer dominates.
2) Heat gain from friction is neglected because radial heat losses to the environment are far more significant and dominate the thermal behavior of the system.
3) Water properties, such as density and specific heat capacity, are considered uniform and constant throughout the simulation. However, the supply and return networks can be modeled separately to account for different operational temperature ranges.
4) The pressure propagation is negligible (Stevanovic et al., 2007), and the hydraulic calculation is based on steady-static method. This allows decoupling hydraulic simulations from thermal simulations for fast simulation.

Consequently, changes in the water temperature profile depend solely on time delay and heat losses to the surroundings.

The DES model tracks the movement of infinitely thin water sections within a pipe. These *water frontiers* act as dynamic sampling points, where their temperatures are essential for determining the water temperature profile. To ensure accurate calculations, key inlet parameters of the water frontiers are recorded, including creation time, temperature, velocity, and distance to adjacent frontiers. The temperature of water frontiers can be calculated directly from their inlet temperature and travel time without numerical errors. The water temperature profile between adjacent water frontiers is estimated by a linear approximation. Therefore, DES model can accurately and efficiently capture the water temperature profiles at any observation node over time, and across spatial locations at any given moment.

2.1 Discrete event simulation

Discrete event simulation (DES) is a dynamic modeling technique that tracks a sequence of chronological events representing instantaneous changes in system state. No state change is assumed to occur between consecutive events; therefore, the simulation time step varies based on the occurrence times of adjacent events. Events can be scheduled, rescheduled, or canceled as needed.

The occurrence of events is managed using an event queue, where events are ordered by their scheduled activation times. The DES simulation engine iteratively removes the earliest event from the queue and executes the corresponding calculations. The simulation terminates automatically when the event queue is empty.

We define three types of events: mass flow rate change event, water frontier arrival events, and inlet temperature change events. Each pipe has its own water frontier arrival event and inlet temperature change event. The entire network, however, shares a single mass flow rate change event, as the mass flow rates for all customers are typically measured simultaneously in most DH networks. The computational procedures for these events are illustrated in Figure 6. Notably, inlet temperature changes can occur either instantaneously or gradually. In the gradual mode, inlet temperature change events define changes in the slope of the piecewise linear inlet temperature function over time.

2.2 Calculation in a single pipe

Accurate simulation within a pipe is essential for achieving accurate DH network simulations. In a Lagrangian model, simulating temperature propagation within a pipe requires precise tracking of the location of water particles and their associated heat losses. Subsection 2.2.1 outlines the principles for tracking the location and travel time of water particles. Subsections 2.2.2 and 2.2.3 detail how to calculate temperatures and heat losses based on the travel time.

2.2.1 Travel time

Figure 2 illustrates an example involves flow reversal, highlighting the processes of scheduling, rescheduling, and canceling arrival events within a pipe. Initially, there are no water frontiers in the pipe. The flow speed changes as a step function.

- At time t_1, an inlet temperature change at the current inlet (left end) initiates the creation of the first frontier F_1, with its arrival time determined by the flow speed $|v_1|$ and pipe length.
- At t_2, when the flow halts, new water frontiers F_2 and F_3 are generated at the inlet and outlet, respectively, and the arrival event for F_1 is canceled.

- At t_3, flow reversal changes the outlet to the left end of the pipe. Frontier F_2 arrives immediately, and F_1 becomes the next water frontier to arrive. Its arrival time is recalculated based on $|v_3|$ and the distance between F_1 and F_2. A new frontier, F_4, is created at the current inlet (right end). Frontiers F_3 and F_4 are positioned infinitesimally close, reflecting a stepwise temperature change.
- At t_4, frontier F_1 reaches the current outlet, and F_3 becomes the next frontier to arrive, with its arrival time scheduled based on $|v_3|$.

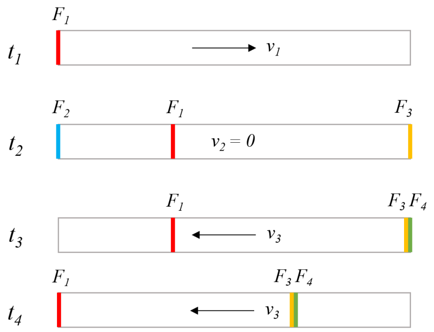

Initial condition:
inlet temperature is T_1 and flow velocity is v_1

t_1: Inlet temperature increases from T_1 to T_2
t_2: Flow stops – velocity changes from v_1 to zero
t_3: Flow reverses – velocity changes from zero to v_3
t_4: Water frontier F_1 arrives at the pipe end

Figure 2 Schematic diagram of a bidirectional flow example.

Assuming incompressible flow, the distance between two water particles remains constant once they enter a pipe. When the mass flow rate remains unchanged between two arrival events, the next scheduled arrival time, $t_{\text{scheduled}}^{(k+1)}$, can be directly calculated based on the distance and the current flow speed, as illustrated in the scenario at t_3. If the mass flow rate changes, however, the next arrival event must be rescheduled based on the updated flow rate and the remaining distance between the next arriving water frontier (F_{Next}) and the outlet. When the flow direction stays the same, the activation time is determined by (1). $t^{(k)}$ represents the current simulation time at step k. $t_{\text{scheduled}}^{(k-1)}$ is the previously scheduled arrival time. $v^{(k-1)}$ and $v^{(k)}$ correspond to the prior and updated speeds, respectively. If the flow direction changes, the outlet changes as well, potentially resulting in a different F_{Next} and requiring arrival event rescheduling. In this case, $t_{\text{scheduled}}^{(k)}$ is calculated using (2), where $t_{\text{in}}^{(F_{\text{Next}})}$ is the creation time of the next arriving water frontier according to current flow direction.

The next water frontier arrival time for a pipe is managed using a double-ended queue (deque) for storing the water frontiers. After updating the next arrival time, the corresponding arrival event is rescheduled in the event queue.

$$t_{\text{scheduled}}^{(k)} = t^{(k)} + (t_{\text{scheduled}}^{(k-1)} - t^{(k)})\frac{V^{(k-1)}}{V^{(k)}} \tag{1}$$

$$t_{\text{scheduled}}^{(k)} = t^{(k)} + (t_{\text{in}}^{(F_{\text{Next}})} - t^{(k)})\frac{V^{(k-1)}}{V^{(k)}} \tag{2}$$

The parameters of the water particle currently at the outlet are updated for temperature calculations. The historical inlet time and the arrival time of the particle are denoted by $t_{\text{in}}^{(k)}$ and $t_{\text{out}}^{(k)}$, respectively, where $t_{\text{out}}^{(k)}$ equals to the current simulation time $t^{(k)}$. The particle's travel time, $\tau^{(k)}$, is given by the difference between the arrival time and the inlet time as shown in (4). $v_{\text{in}}^{(k-1)}$, $t_{\text{in}}^{(k-1)}$, and $t_{\text{out}}^{(k-1)}$ refer to the historical inlet flow speed, historical inlet time, and arrival time of the previously arrived sampling frontier.

Using the recorded inlet parameters of water frontiers, the travel time for any particle can be calculated accurately. The travel time of water particles forms a piecewise linear function, with breakpoints occurring at moments of flow speed changes.

$$t_{\text{in}}^{(k)} = t_{\text{in}}^{(k-1)} + (t_{\text{out}}^{(k)} - t_{\text{out}}^{(k-1)})\frac{V^{(k-1)}}{V_{\text{in}}^{(k-1)}} \tag{3}$$

$$\tau^{(k)} = t_{\text{out}}^{(k)} - t_{\text{in}}^{(k)} = \tau^{(k-1)} + (1 - \frac{V^{(k-1)}}{V_{\text{in}}^{(k-1)}})(t_{\text{out}}^{(k)} - t_{\text{out}}^{(k-1)}) \tag{4}$$

2.2.2 Temperature calculation

The temperatures of water particles change as the water travels from the heating plant to customers due to heat transfer between the water and its surroundings. Depending on the network structure, pipe dimensions, and operating conditions, heat loss during transmission can account for 5% to 20% of the annual heat supply (Sartor & Dewalef, 2017). Consequently, the effect of heat loss on water temperature during transit cannot be overlooked.

The DES model incorporates distinct temperature equations for different pipe types, including single pipe, parallel single pipes, and twin pipes, as illustrated in Figure 3. Here, q_h and q_c represent the heat losses from hot pipe and cold pipe, respectively. The formulas for heat loss, $q_{\text{s}\to\text{g}}$, are based on the study (Wallentén, 1991), which accounts for the coupled influence of ground temperature and the water temperature in parallel pipes.

In the Lagrangian approach, heat loss depends only on time, as the spatial coordinate is omitted when the observer follows moving water particles. Differential equation (5) describes the relationship between temperature and heat loss. Its solution, equation (6), reveals that temperature is an exponential function of travel time τ in the pipe. Here, T_{in} is the inlet temperature recorded when the water frontier is created.

The coefficients of k_1 and k_2 for different pipes are summarized in Table 2. T_g is the ground surface temperature, while T_p refers to the corresponding temperature in the other parallel pipes. λ_i and λ_g are heat conductivity of insulation and soil respectively. C refers to the overall heat capacity of water and is equivalent to $\rho c_p A$. ρ and c_p are the density and specific heat capacity of water. A is the cross-secessional area of the pipe. The detailed formulas for T_s, T_a, R, R_s, R_a, h_s, and h_a are provided in Appendix 1.

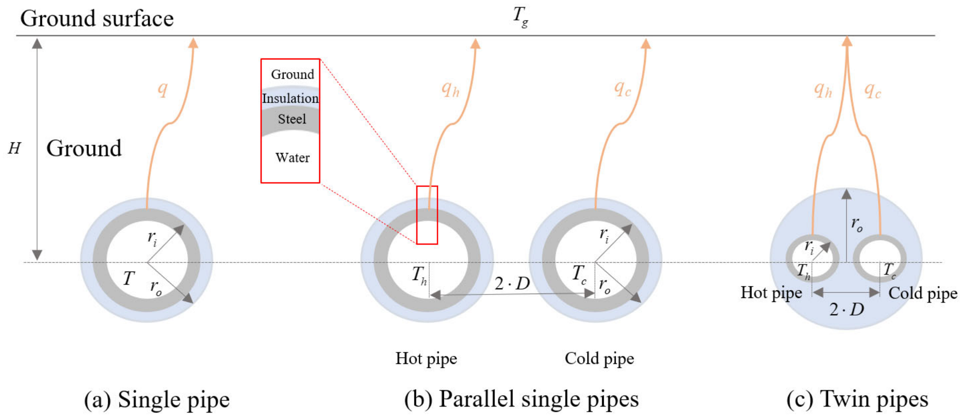

Figure 3 Heat loss from the pipe wall to ground surface for different pipes.

$$\rho c_p A \frac{dT(t)}{dt} = -q_{s \to g} \tag{5}$$

$$T(\tau) = \left(T_{\mathrm{in}} - k_2\right) e^{k_1 \tau} + k_2 \tag{6}$$

Table 2 Different coefficients k_1 and k_2 in the outlet temperature formulas.

Pipe types	(a) Single pipe	(b) Parallel single pipes	(c) Twin pipes
k_1	$-\frac{1}{CR}$	$-\frac{R_s + R_a}{2CR_s R_a}$	$-\frac{\pi \lambda_i \left(h_s + h_a\right)}{C}$
k_2	T_g	$\frac{\left(R_s - R_a\right) T_p + 2R_a T_g}{R_s + R_a}$	$\frac{\left(h_a - h_s\right) T_p + 2h_s T_g}{h_s + h_a}$

2.2.3 Energy calculation

Heat loss can be calculated either directly from the temperature drop of particles or indirectly through an energy balance. In this model, we use the energy balance method, as shown in Figure 4, with the reference temperature set to ground temperature. The heat loss calculation is an optional feature in this model.

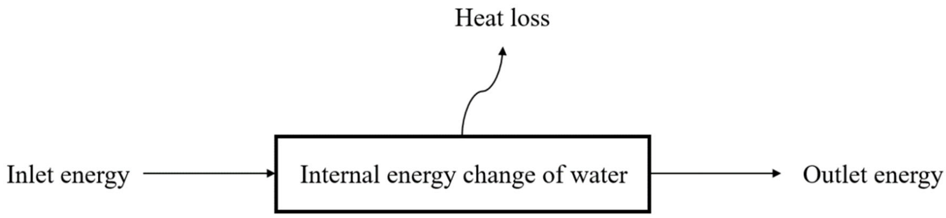

Figure 4 Energy balance of pipe during simulation.

The inlet energy Q_{in}, outlet energy Q_{out}, internal heat energy E, and heat loss of each pipe Q_{loss} can be computed from (7)-(10). L is the pipe length. Assuming linear temperature profile between breakpoints simplifies the integrals.

$$Q_{\text{in}} = \rho c_w A \int_{t_0}^{t_{\text{end}}} v(t)\left(T_{\text{in}}(t) - T_g\right) dt \tag{7}$$

$$Q_{\text{out}} = \rho c_p A \int_{t_0}^{t_{\text{end}}} v(t)\left(T_{\text{out}}(t) - T_g\right) dt \tag{8}$$

$$E(t) = \rho c_p A \int_0^L \left(T(t,x) - T_g\right) dx \tag{9}$$

$$Q_{\text{loss}} = Q_{\text{in}} - Q_{\text{out}} - (E(t_{\text{end}}) - E(t_{\text{start}})) \tag{10}$$

2.3 Network modeling

The network model is an object-oriented framework composed of pipe and node objects, where pipes are connected through nodes. Nodes are divided into two main categories: leaf nodes and internal nodes. Leaf nodes, which have a single connected edge, correspond to customers or production sites. Internal nodes act as junctions between two or more DH pipes and are further classified into straight-line nodes and forking nodes. Straight-line nodes connect exactly two pipes, while forking nodes connect three or more pipes. Forking nodes are further divided into splitting nodes, characterized by single inflow with multiple outflows, and merging nodes, characterized by multiple inflows.

The calculations within the pipe objects have been detailed in the previous section. This section focuses on the interaction between nodes and pipes. This interaction is crucial for accurately capturing temperature dynamics across the network, especially in scenarios with varying flow directions or at merging and splitting nodes.

Assuming fully mixed water, the water temperature at any node j equals to the average inflow temperature weighted by mass flow rate, m. The inflow temperature calculated from the flows arriving from its upstream pipes. The mixing temperature can be calculated using (11), where I_{in}^{j} represents the set of pipes with inflow to the node j.

$$T_{\text{mix}}^{j} = \frac{\sum_{i \in I_{\text{in}}^{j}} |m_i| T_{\text{out}}^{i}}{\sum_{i \in I_{\text{in}}^{j}} |m_i|} \tag{11}$$

When water frontiers reach the end of a pipe, they are removed and re-created in the downstream pipes, adopting the temperature of the corresponding node. If the node is a splitting node (with only one inflow), the node temperature equals the outlet temperature of its upstream pipe. Conversely, for a merging node, the node temperature is determined by the mixing temperature.

Figure 5 illustrates a scenario where the flow direction in Pipe 1 reverses. Although the water temperatures at the ends of Pipe 1 remain unchanged at this instant, the mixing temperatures are altered due to changes in the inflows. Consequently, extra water frontiers are generated not only in the reversed pipe but also in the former downstream pipe (Pipe 3) and the new downstream pipe (Pipe 0) to track instantaneous temperature changes.

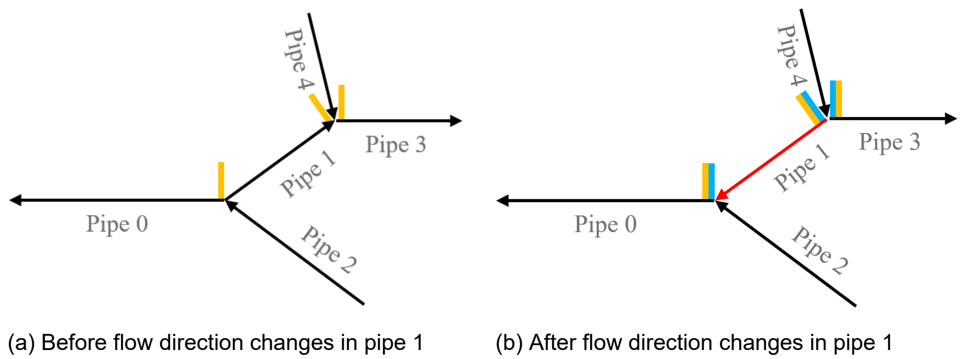

Figure 5 Water frontiers generation in adjacent pipes when a flow changes direction.

Figure 6 depicts the DES flowchart for simulating meshed DH networks. While water frontier arrival and inlet temperature change events involve localized updates in a single pipe or a few adjacent pipes, mass flow rate changes require updates across nearly the entire network. Hydraulic simulations are performed before thermal simulations to determine the mass flow rates in all pipes.

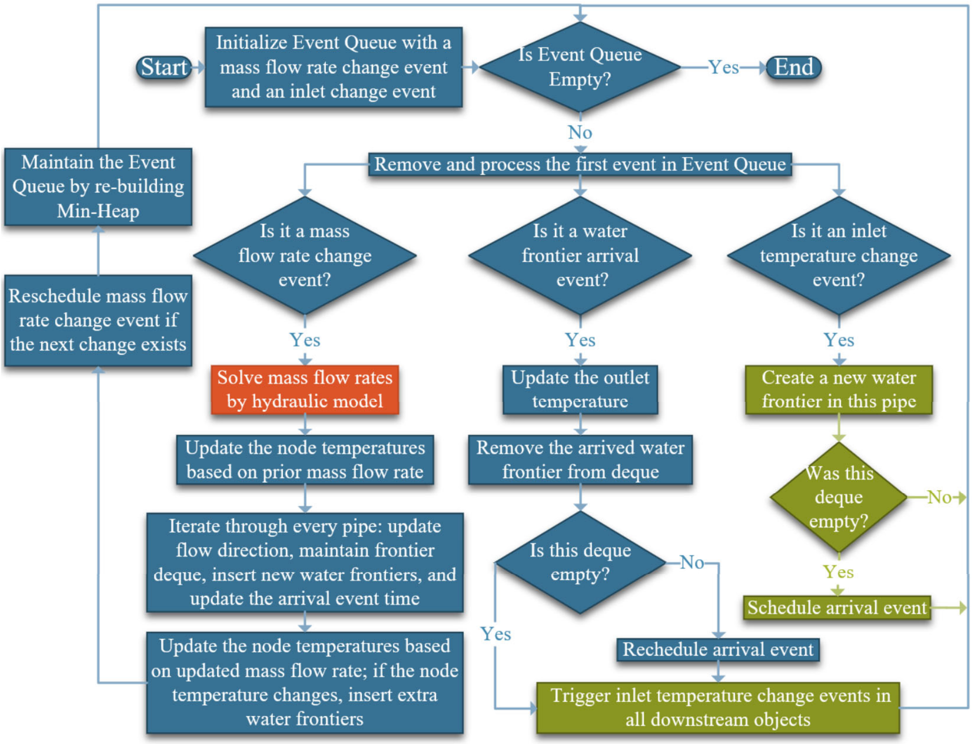

Figure 6 DH Network modeling based on Discrete Event Simulation.

The core challenge in hydraulic simulation for meshed networks is solving a system of equations. This system is derived from mass balance (12) and Kirchhoff's second law (13), which states that the directed sum of potential pressure differences around any closed cycle must equal zero. The term m_j^b represents the mass flow rate specified as a boundary condition at customer and production site nodes, which is zero at internal nodes. Positive values correspond to inflow into the system, while negative values denote outflow. I_j denotes the set of pipes connected to node j, and m_i is the mass flow rate in pipe i. The value of m_i is positive when the flow follows the nominal direction and negative when it opposes it, with the sign indicating nominal inflow (positive) or nominal outflow (negative).

$$m_j^b + \sum_{i \in I_j} \pm m_i = 0 \text{, for any node } j \tag{12}$$

$$P_c = \sum_{i \in c} \pm \Delta p_i(m_i) = 0 \text{, for any cycle } c \tag{13}$$

The pressure drop Δp in each pipe is calculated using the Darcy-Weisbach equation (14), with the friction factor f depending on flow conditions. For turbulent flow (Re≥4000), an explicit approximation is used for f instead of the implicit

Colebrook-White equation, as suggested by (Yıldırım, 2009). Here, Re denotes the Reynolds number. D_w is the diameter of the pipe's inner wall. ε is to the absolute roughness of pipe wall. Linear interpolation is used for transitional flow (2000<Re<4000).

The nonlinear pressure drops in pipes make the overall problem nonlinear. However, since flow adjustments along cycles has no impact on the mass balance at nodes, the original problem can be decomposed into a linear problem and nonlinear subproblems for each cycle block, defined as the transitive closure of dependent cycles. The linear problem is addressed by assigning arbitrary values to the flows in the cut-off edges of all cycles, effectively reducing the meshed network to a tree. This linear problem only needs to be solved once per time step, while the nonlinear subproblems require iterative calculations. Newton-Raphson method is employed to solve the nonlinear subproblems, which can be addressed independently for each cycle block. This decomposition has the potential to accelerate hydraulic simulations in large-scale networks with complex topologies. A detailed description of the hydraulic model is provided in publication III.

$$\Delta p(m) = p_{\text{origin}} - p_{\text{target}} = Lf\rho\frac{v|v|}{2D_w} = Lf\frac{m|m|}{2D_w\rho A^2} \tag{14}$$

$$f = \begin{cases} 64/Re, \ \ Re \leq 2000 \\ [0.8686\ln(0.4587\,Re/S^{\frac{S}{S+1}})]^{-2}, S = \frac{0.124\,\varepsilon\,Re}{D_w} + \ln(0.4587\,Re), Re \geq 4000 \end{cases} \tag{15}$$

2.4 Implementation optimization

The event-driven nature of DES can lead to high computational costs, especially when managing numerous events and frequently updating the event queue. This issue becomes pronounced in large-scale DH network simulations, necessitating efficient techniques to optimize performance. We propose three strategies to improve computational speed. To ensure broad compatibility across different operating systems and platforms and achieve fast simulations, the entire model was developed using C++.

2.4.1 Lazy evaluation

Lazy evaluation defers computations until their results are required, improving both speed and memory efficiency. In DES model, this approach calculates travel time, outlet temperature, and energy only when necessary. The water frontiers are only updated when they arrive the pipe end. Simultaneous updates occur only when mass flow rate changes. This approach allows each pipe to operate on independent time steps, avoiding redundant intermediate calculations and ensuring accurate breakpoint tracking for water temperature profiles. By limiting updates and calculations to essential scenarios, this strategy significantly optimizes the efficiency of each computational step.

Downstream pipes also benefit indirectly, as fewer updates in upstream outlet conditions lead to reduced water frontier generation in downstream pipes, thereby dramatically decreasing the number of water frontier arrival events.

2.4.2 Customized priority queue

A priority queue is a data structure that manages elements with priorities, where the highest-priority element (earliest event time in event queue) is processed first. This structure is essential for chronological event management in DES.

To optimize the event queue, three strategies are applied to reduce unnecessary updates. First, inlet temperature change events for pipes with internal-node inlets are omitted, as these are linked to upstream pipe arrival events. Each pipe has a single event, except the supply pipe connected to the heating plant. Second, the queue is updated only once when two water frontiers arrive simultaneously. Third, customer demand changes occurring at the same time are processed together.

A Min-Heap, a complete binary tree enabling insertion and root deletion in $O(\log n)$ time, is used to implement the priority queue. Although the C++ standard library provides a Min-Heap, it does not fully meet DES network requirements, particularly for event rescheduling. To address this, a customized Min-Heap was developed with the following enhancements:

- Efficient handling of event rescheduling by delaying heap maintenance until all simultaneous updates are complete. This is important for mass flow rate change event, since most arrival events need to be rescheduled.
- An indexing scheme enabling $O(1)$ element access (not limited to the root), eliminating the need for $O(n)$ direct search during event rescheduling.
- Fixed heap size to accommodate the maximum number of active events (number of pipes + number of heating plants + 1). Using static array to implement the heap avoids the overhead associated with dynamic memory allocation during runtime.

These improvements make the customized Min-Heap more efficient than the standard implementation, particularly for event rescheduling and element searching.

2.4.3 Tolerance threshold for redundant water frontiers

Redundant water frontiers, which have minimal impact on the temperature profile, can be eliminated to improve simulation efficiency by reducing temperature computations and event queue updates. While capping the number of water frontiers in each deque is one approach, it can introduce numerical errors due to forced merging (Oppelt et al., 2016).

We propose a tolerance threshold method to address this issue. This approach sets a threshold for creating new water frontiers based on the disparity between computed and interpolated outlet temperatures. Figure 7 illustrates a scenario where a new water frontier, F_*, is expected to be created in downstream pipes when the mass flow rate changes. The computed outlet temperature of F_* is calculated from its travel time and the interpolated inlet temperature base on inlet temperatures of F_0 and F_1. The interpolated outlet temperature of F_* is calculated using outlet temperatures of previously arrived frontier F_0 and the next scheduled arriving frontier F_1. The estimated outlet temperature of frontier F_1 is obtained by assuming an unchanged flow speed before its arrival. If this disparity falls below the threshold, the new frontier is omitted in downstream pipes.

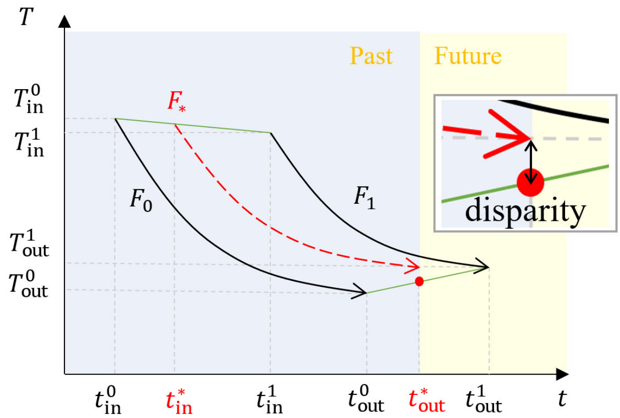

Figure 7 The disparity between computed and interpolated outlet temperatures.

The threshold ensures that only significant changes in temperature profiles trigger new water frontiers. Eliminating a single frontier also prevents the propagation of future frontiers in all downstream pipes associated with it. Choosing an appropriate threshold is crucial for balancing accuracy and computational performance—overly high thresholds risk omitting key events, while overly small thresholds may offer minimal performance gains.

3 Numerical studies

Before DES model is integrated to DH system for real applications, its performance in predicted accuracy and simulation efficiency must be validated. In Publications I – III, DES model was validated with measurements from three real applications: a single-pipe, a tree-shaped network, and a meshed network, respectively.

3.1 Validation

The 24-hour single-pipe case study in publication I aims to test the model's accuracy in simulating water temperature and heat loss within a pipe. The investigated pipe is part of a real network in Shijiazhuang, China, with a length of 9250 m and an inner diameter of 1400 mm. During the measurement period, the inlet temperature ranged from 88.4 to 97.9 °C, while the flow rate varied between 9012.4 and 9761.8 m^3/h. Measurements were taken at approximately 5-minute intervals. Four models with different inlet temperature assumptions and interpolation methods were proposed. Their simulated outlet temperatures were compared with measurements, and a numerical comparison among the models was performed. The results support the use of linear approximation in future studies.

The case study in publication II focuses on a tree-shaped network with a central heating plant, part of the Pohja network located in Uusimaa, Finland. This network supplies water for domestic hot water and space heating to 24 customers, including commercial buildings, apartment buildings, and detached houses. The network comprises 102 pipes after integrating the pipes with same properties. The supply and return pipes are installed in parallel, either as separate single pipes or as twin pipes, corresponding to types (b) and (c) in Figure 3 . Simulations were conducted for both the supply and return sides, and the simulated node temperatures were compared with measured supply temperature of customers. This study used 72 days of hourly measurements and aimed to validate the temperature propagation calculations at splitting nodes and the mutual heat transfer between supply and return pipes.

Publication III investigates a meshed network in Huanghua, China, featuring two cycles, two heating plants, and 186 pipes (after pipe integration). The layout of the investigated network is shown in Figure 8. This network provides space heating for 86 substations, including one abundant substation with zero flow. The main heating plant operated throughout the 85-day study period, while the peak boiler operated for 487 hours. The study period also included the start-up and shut-down phases of the peak boiler. When the peak boiler was inactive, the flow directions remained stable, as indicated by the arrows in Figure 8. During off-peak periods, flows merged at nodes 128 and 162. However, during peak boiler operation, the flow directions in the pipes within the two cycles changed. Pipes experiencing flow reversal are highlighted in red in Figure 8. Using hourly measurements of mass flow rates at leaf nodes and supply temperatures at the heating plants, the temperatures at substations were calculated and compared with measured values. The simulation for supply network aimed to validate the thermal simulation for flow direction reversals and water mixing at merging nodes. Validating a meshed network with multiple heating sources is more complex than a tree-shaped network due to uncertain flow distribution. Accurate thermal simulation requires precise hydraulic calculations, which impact merging nodes in terms of their locations and mixing temperatures. In addition to proper parameter settings, high-quality measurements of mass flow rates at leaf nodes (heating sources and substations) are important. We filled missing data for two substations using a long short-term memory (LSTM) model trained on measurements from another period. To address discrepancy between total supplied and delivered mass flow rates, we applied a least-squares method to adjust the supplied mass flow rates of heat sources.

Despite appropriately setting model parameters based on available network data, temperature discrepancies were observed at most substations. These discrepancies, evaluated as the time-weighted average temperature difference between simulated results and measurements, showed no strong correlation across substations or water temperatures, and remained consistent during both off-peak and peak periods. Potential causes include incorrect heat meter calibration or operational issues such as misconnected supply and return pipes or water leakage. However, the consistency of these offsets allowed us to apply a vertical temperature shift for validation.

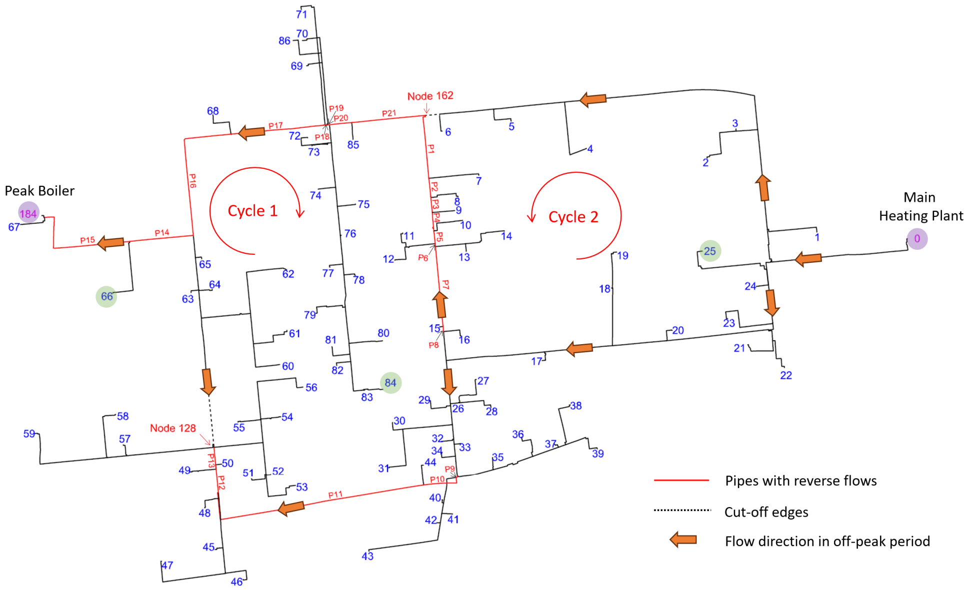

Figure 8 Layout of the investigated DH network in publication III.

Figure 9 presents detailed results for three representative nodes in the meshed network: two near the heat sources (nodes 25 and 66) and one at the farthest point in a long branch (node 84). These nodes were selected to capture distinct hydraulic and thermal conditions within the network. Node 25 received water solely from the main heating plant throughout the study period, providing a baseline for evaluating the model under stable flow conditions. In contrast, Node 66, located near the peak boiler, experienced significant changes in water source depending on the operational period—receiving water from the main heating plant during off-peak periods and from the peak boiler during peak periods. This scenario highlights the model's capability to handle sudden flow reversals. Node 84, representing a more complex scenario, encountered varying water sources during peak periods, receiving water either entirely from the main heating plant, entirely from the peak boiler, or from a mixture of both. Even during off-peak periods, when water was fully supplied by the main heating plant, accurate simulation remained challenging due to the mixing of water from different paths. The results show that although localized discrepancies are observed, such as the error around December 15th, simulated temperatures align well with measurements most of time.

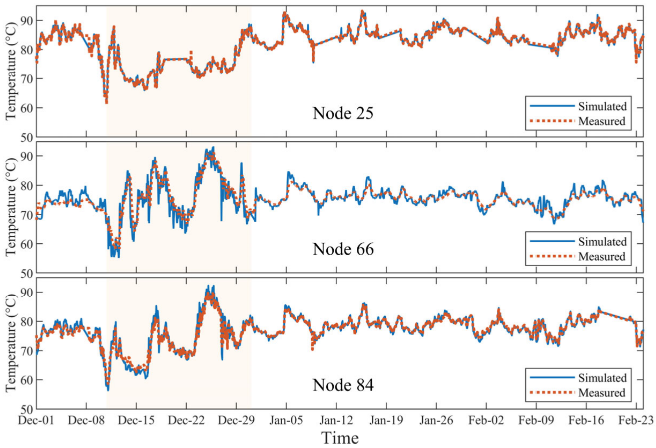

Figure 9 Comparison of measured and simulated node temperatures for the investigated period (yellow shaded area indicates peak period).

Table 3 summarizes the overall performance indicators of the DES model across the three case studies. ME and RSD refer to the mean error and residual standard deviation of the simulated node temperatures, respectively. By comparing simulated node temperatures with measurements in each case, we conclude that the model is reliable and robust.

Table 3 Summary of three case studies.

Case studies	ME [°C]	RSD [°C]	Simulation time
I: 24-h simulation for a single pipe	-0.01	0.16	59 µs
II: 72-day simulation for a tree-shaped network with 24 customers and 102 pipes	0.43	0.61	0.219 s
III: 85-day simulation for a meshed network with 86 substations, 2 heating plants, 186 pipes, and 2 cycles	0.00	1.15	0.29 s

* ME and RSD in cases II and III refer to the average values of all customers/substations.

3.2 Computational speed

Table 3 provides an overview of the simulation times for the three case studies. To further understand the factors influencing computational speed, we analyzed the relationship between simulation time and the number of water frontiers (sampling points), as shown in Figure 10. In both cases, simulation time increases linearly with the number of water frontiers. This highlights the importance of efficiently selecting sampling points to enable faster modeling. The proposed threshold tolerance approach that eliminates redundant water frontiers—those with an insignificant impact on the accuracy of temperature profiles—can improve computational speed without sacrificing temperature accuracy.

The slopes of the two lines indicate that the meshed network model presented in publication III is asymptotically faster at simulating the same amount of water frontiers. This improvement in computational speed is attributed to the re-designed implementation described in publication III.

Additionally, the results reveal a noticeable positive intercept for the meshed network simulation, in contrast to the near-zero intercept for the tree-shaped network simulation. This difference is due to the computationally intensive hydraulic simulation required for meshed networks. The findings suggest that computational speed is primarily determined by the thermal simulation, with hydraulic simulation accounting for 25.7% of the total simulation time in the meshed network case study using the recommended enhanced model.

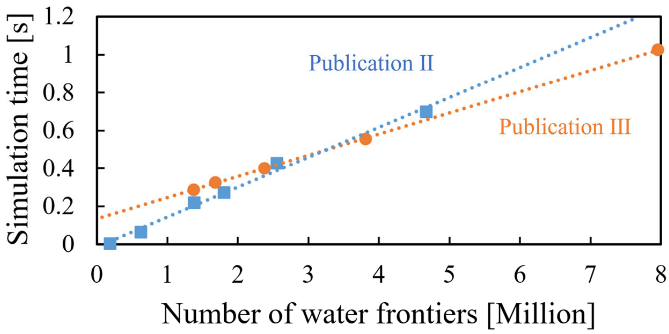

Figure 10 Relationship between the simulation time and number of water frontiers.

4 Research contributions

This study introduces a novel method based on discrete event simulation (DES) for dynamic modeling of district heating (DH) networks with variable time steps. It can be widely applied to modern DH networks with complex network topologies and advanced operational strategies, such as "variable flow, variable temperature". The developed DES model offers both accuracy and computational efficiency, making it particularly suitable for online system optimization in DH systems that require intensive iterative calculations. For scalability and rapid simulation of large-scale networks, DES model is implemented in C++.

The research is structured around three publications (I – III), each addressing a key challenge in developing the DES model. These challenges include establishing the theoretical foundation, implementing the model efficiently, and ensuring its scalability and applicability to various network topologies. Together, the publications outline a step-by-step progression in developing the DES network model from scratch.

4.1 Publication I

Holistic optimizing DH systems is often impeded by the computational complexities associated with network modeling and the existing approaches are either slow or inaccurate. This inspires us to develop an innovative method to address the bottleneck in computational efficiency. The main contribution of publication I is to answer the question what the critical sampling points for accurate prediction of water temperature profile within a pipe are. This guides its efficient implementation of variable time step simulation.

A single-pipe model based on unidirectional flow with four computational modes was developed and validated using real measurements. The results demonstrated that, for the same simulation, the DES model achieved a comparable level of temperature accuracy while being 593 times faster than the characteristic line model and 1288 times faster than the implicit upwind model (Y. Wang et al., 2017).

Additionally, three fundamental conclusions support subsequent studies. First, the travel times of water particles exhibit a piecewise linear relationship when water speed changes instantaneously. This results in piecewise exponential temperature profiles when the inlet temperature changes instantaneously or exponentially. Second, approximating the exponential temperature profile between breakpoints using linear interpolation is both computationally efficient and accurate under normal operational conditions. Third, the gradual temperature change assumption provides a more accurate representation of water temperature profiles compared to the instant temperature change assumption. These findings support the use of linear approximation between water frontiers in following studies.

4.2 Publication II

The accuracy and efficiency of thermal simulation within a pipe was validated in publication I. In publication II, the DES model was extended for application in tree-shaped networks utilizing an object-oriented framework comprising pipes and nodes. This extension addresses the management of multiple pipe calculations, the propagation of water frontiers throughout the network, and the mutual heat transfer between supply and return pipes.

Another key contribution is the optimization of the DES model's implementation. Due to its event-driven nature, DES can become computationally expensive, particularly when managing a large number of events and frequent updates. To mitigate this issue in large-scale network simulations, we employed three advanced techniques for faster simulation: lazy evaluation, a customized priority queue, and a tolerance threshold.

The DES network model was validated and tested using 72 days of measurements from a network containing 102 pipes. In this case study, the tolerance threshold method proved highly effective, significantly reducing the number of sampling points to expedite calculations with negligible accuracy degradation. This optimization resulted in a 69% speed improvement, completing the 72-day simulation in just 0.219 seconds. Furthermore, the results demonstrated that the computation time is linearly dependent on the number of sampling points, highlighting the potential scalability of the DES model for large-scale networks.

4.3 Publication III

In tree-shaped networks, the mass flow rates throughout the network can be determined based on mass flow balance equations, provided the mass flow rates of the leaf nodes (customers) are known. Additionally, the flow direction in each pipe is fixed, always running from the heating plant to customers. However, meshed networks are increasingly adopted in modern DH systems for their improved reliability, flexibility, and ability to handle multiple heat sources. To accommodate broader applications, the DES network model was extended from tree-shaped networks to meshed networks with multiple heating plants in publication III.

In meshed networks, flow directions along cycles vary with hydraulic conditions, requiring the mass flow distribution to be solved using additional pressure balance equations based on Kirchhoff's second law. Hydraulic conditions influence the merging locations of flows but also the mixing temperatures at merging nodes, which are affected by the mass flow rate contributions from inflows with different temperatures. Therefore, solving the hydraulic conditions is essential for thermal simulations. However, hydraulic calculation can be solved independently of thermal simulations because pressure-related water parameters change minimally within the operating temperature range (H. Wang & Meng, 2018).

This study contributes in two significant ways. First, the pipe model was extended to handle bidirectional flows, enabling the simulation of reverse flows commonly observed in meshed networks. Second, a hydraulic model based on the Newton-Raphson method was developed and integrated with the previous DES thermal model, resulting in a quasi-dynamic hydraulic-thermal DES model. Additionally, the mass flow rate change event calculation was redesigned to accommodate the dynamic changes in flow.

The model's accuracy in temperature prediction and computational efficiency were validated using measurements from a meshed network with multiple heating plants, comprising 186 pipes and two dependent cycles. Simulated temperatures closely matched the measurements. For an 85-day simulation, the DES model required just 0.29 seconds, with hydraulic simulations accounting for 25.7% of the total computation time. Furthermore, the finding from publication II—that computation time increases linearly with the number of sampling points—was confirmed in this meshed network case study.

5 Answers to research questions

This section addresses the six research questions outlined in Section 1.4.

1) Strategic selection and dynamic updates of sampling points are achieved by placing them where the temperature profile is not differentiable. The time step is automatically determined based on when these specific sampling points require updates.
2) Heat loss calculations use formulas that account for the water temperature in parallel pipes. Temperature-related coefficients are updated hourly based on the average historical inlet and outlet temperatures of the parallel pipe.
3) In the DES framework, variable time step simulation is implemented using a lazy evaluation approach. Each pipe object operates on its own adaptive time step, managed by an independent deque. A global event queue, organized using a heap, controls the simulation timeline. At each event, only the affected objects are updated, and the heap is partially adjusted. Skipping updates for unaffected objects allows the simulation to advance efficiently. This ensures that computations are performed only when necessary, reducing computational cost while preserving model fidelity.
4) The DES model captures the thermal and hydraulic dynamics of the DH network with sufficient accuracy for engineering applications. The accuracy of thermal dynamics depends on the accuracy of hydraulic dynamics, which is influenced by data quality.
5) Computational speed scales linearly with the number of sampling points in the test networks. Assuming this characteristic holds for large-scale networks, the model can complete 24-h simulation in 10 minutes for a network with 63.2 million pipes, making it suitable for system optimization.
6) The model can be further speeded up by monitoring only the sampling points that significantly impact temperature profiles while omitting those with minor effects.

6 Discussion and conclusion

6.1 Innovations and comparative analysis

This research develops an accurate and efficient Lagrangian district heating (DH) network model with variable time steps using discrete event simulation (DES). It provides a solid theoretical foundation for correctly employing variable-step simulation and demonstrates its efficient implementation through DES. Six distinctions from existing models can be identified, representing the main innovations that decreases numerical errors while ensuring computational efficiency in DH network simulations:

1) Precise calculation of travel time: Dynamically defined temporal and spatial discretization eliminates numerical errors in water particle travel time, ensuring accurate thermal simulations.
2) Thermal calculation without numerical diffusion: Sampling points are defined as infinitely thin water sections, preventing numerical diffusion seen in fully mixed control volume methods.
3) Identification of the essential sampling points: Instead of monitoring the status changes with constant frequency, we identified critical sampling points to ensure that all significant temperature changes are accurately recorded. Intermediate temperature variations are effectively captured using linear interpolation, which approximates the exponential temperature profiles with high precision.
4) Variable time step simulation with lazy evaluation: Our approach updates only essential data at key time points (e.g., water temperature at pipe ends) and applies interpolation selectively, enhancing both speed and accuracy.
5) Adaptive local updates: The model assigns different time steps to different pipes, enabling real-time adjustments. It does not require preliminary trial simulations to determine optimal time steps. This adaptability reduces computational overhead while maintaining accuracy.
6) Reliable solution for fast simulation: Our model with tolerance threshold offers a robust solution for balancing computational speed and accuracy. The introduced errors are predictable and well-controlled, ensuring reliability for practical applications.

Researchers have put extensive efforts to improve the accuracy of district heating models by refining their complexity. Examples include adopting fully-dynamic models to account for pressure wave effects (Guo et al., 2023; Y. Wang et al., 2023), employing two-dimensional soil models (del Hoyo Arce et al., 2018), considering the impact of boundary layer near pipe walls on heat transfer (Chertkov & Novitsky, 2019; Dénarié et al., 2019), or using higher-order numerical methods (H. Wang & Meng, 2018; Zheng et al., 2020). While these approaches aim to enhance model precision through more detailed calculations, they often overlook the impact of numerical errors.

In practice, comparisons with measured data show that these refined models demonstrate no significant advantages over simpler one-dimensional plug flow models. Additionally, the refined models are typically impractical due to their reliance on highly detailed input parameters. In real-world networks, our knowledge of many pipe segment properties is limited, and parameters such as burial depth or insulation thermal conductivity are often estimated based on design guidelines. This increased complexity makes model calibration more challenging and offers limited improvements in accuracy, further reducing the practicality of such approaches.

Furthermore, our comparisons relying on measured data across a single pipe, a tree-shaped network, and a meshed network demonstrates that even basic heat loss equations can achieve highly reliable results. This finding underscores that focusing on key physical principles and minimizing unnecessary complexity allows simpler models to provide more feasible and efficient solutions for DH networks without compromising accuracy. Additionally, our results highlight that well-designed physical models can outperform data-driven approaches in both efficiency and accuracy, as evidenced by a comparison with a data-driven model (Guo et al., 2023).

6.2 Limitation and future research

Ignoring the axial mixing and thermal diffusion can simplify and expedite the simulation. However, these assumptions can sometimes result in distorted temperature profiles, potentially explaining the amplified fluctuations observed in the predicted temperatures compared to measurements. While these unrealistic fluctuations may not significantly affect the average temperature accuracy, they could cause unnecessary and frequent adjustments to the control system in future optimization studies. Consequently, future work should explore methods to smoothen temperature profiles and improve model accuracy.

Incorrect mass flow rate inputs for end users yield a more pronounced impact on temperature accuracy in meshed networks than in tree-shaped networks. As reported in Publication III, errors in mass flow rate data can cause localized or temporary distortions in simulated temperature profiles. However, such inaccuracies in measurements are almost unavoidable in real-world applications. The current hydraulic model is based on solving a determined system, necessitating data preprocessing to balance mass flow rates before simulation. This preprocessing is challenging because the errors are typically unknown. Future research should aim to expand the hydraulic model to accommodate overdetermined systems, integrating additional measurements and enabling the development of advanced hydraulic calibration techniques to improve thermal accuracy.

Additionally, the hydraulic model should be extended to incorporate pressure-regulating devices such as water pumps, check valves, and gate valves. In large-scale DH networks, these pressure-regulating devices might be installed along the cycles. This introduces additional constraints or changes to the network topology, increasing the difficulty of solving hydraulic conditions. Further research is required to enhance the computational efficiency of hydraulic calculations.

The current DES model supports bidirectional flow simulation; however, the flow direction in pipes connected to leaf nodes (customers or heating plants) is fixed. This limitation restricts its application in 5GDHC networks with prosumers. Therefore, extending the model to allow flexible flow directions at the leaf nodes is planned for future work.

While the current model shows promise in terms of scalability, comprehensive testing on large-scale networks is necessary to ensure its practicality and efficiency. A longer-term objective should involve embedding the DES model within an online operational optimization framework for DH systems. Beyond using measurement data as input for monitoring the system's status, the model could be integrated with forecasting approaches like (Hua et al., 2024), to support future planning. Such integration would enable the efficient management of intensive iterative network calculations necessary for system optimization, while fostering smarter and more sustainable heating solutions.

References

Benonysson, A. (1991). *Dynamic Modelling and Operational Optimization of District Heating Systems*. Technical University of Denmark.

Bergsteinsson, H. G., Vetter, P. B., Møller, J. K., & Madsen, H. (2022). Estimating temperatures in a district heating network using smart meter data. *Energy Conversion and Management*, *269*, 116113. https://doi.org/10.1016/j.enconman.2022.116113

Betancourt Schwarz, M., Mabrouk, M. T., Santo Silva, C., Haurant, P., & Lacarrière, B. (2019). Modified finite volumes method for the simulation of dynamic district heating networks. *Energy*, *182*, 954–964. https://doi.org/10.1016/j.energy.2019.06.038

Blazek, J. (Ed.). (2005). *Computational Fluid Dynamics: Principles and Applications* (Second Edition). Elsevier Science. https://www.sciencedirect.com/science/article/pii/B9780080445069500035

Boghetti, R., & Kämpf, J. H. (2024). Verification of an open-source Python library for the simulation of district heating networks with complex topologies. *Energy*, *290*, 130169. https://doi.org/10.1016/j.energy.2023.130169

Brown, A., Foley, A., Laverty, D., McLoone, S., & Keatley, P. (2022). Heating and cooling networks: A comprehensive review of modelling approaches to map future directions. *Energy*, *261*, 125060–125060. https://doi.org/10.1016/j.energy.2022.125060

Calise, F., Cappiello, F. L., Cimmino, L., Dentice d'Accadia, M., & Vicidomini, M. (2023). A comparative thermoeconomic analysis of fourth generation and fifth generation district heating and cooling networks. *Energy*, *284*, 128561. https://doi.org/10.1016/j.energy.2023.128561

Chertkov, M., & Novitsky, N. N. (2019). Thermal Transients in District Heating Systems. *Energy*, *184*, 22–33. https://doi.org/10.1016/j.energy.2018.01.049

Dahm, J. (2001). District Heating Pipelines in the Ground—Simulation Model. *Chalmers University of Technology*, 22.

del Hoyo Arce, I., Herrero López, S., López Perez, S., Rämä, M., Klobut, K., & Febres, J. A. (2018). Models for fast modelling of district heating and cooling networks. *Renewable and Sustainable Energy Reviews*, *82*, 1863–1873. https://doi.org/10.1016/j.rser.2017.06.109

Dénarié, A., Aprile, M., & Motta, M. (2019). Heat transmission over long pipes: New model for fast and accurate district heating simulations. *Energy*, *166*, 267–276. https://doi.org/10.1016/j.energy.2018.09.186

Dénarié, A., Aprile, M., & Motta, M. (2023). Dynamical modelling and experimental validation of a fast and accurate district heating thermo-hydraulic modular simulation tool. *Energy*, *282*, 128397. https://doi.org/10.1016/j.energy.2023.128397

European Commission. Directorate General for Energy. (2024). *Financial instruments and models for heating and cooling: Investors dialogue on energy*. Publications Office. https://data.europa.eu/doi/10.2833/654652

European Commission. Directorate General for Energy, E-Think, TU Wien, Fraunhofer ISI, Öko Institut e.V, & Viegand Maagoe. (2022). *Renewable space heating under the revised Renewable Energy Directive: ENER/C1/2018 494 : final report*. Publications Office of the European Union. https://data.europa.eu/doi/10.2833/525486

Falay, B., Schweiger, G., O'Donovan, K., & Leusbrock, I. (2020). Enabling large-scale dynamic simulations and reducing model complexity of district heating and cooling systems by aggregation. *Energy*, *209*, 118410. https://doi.org/10.1016/j.energy.2020.118410

Giraud, L., Baviere, R., Vallée, M., & Paulus, C. (2015). *Presentation, Validation and Application of the DistrictHeating Modelica Library*. 79–88. https://doi.org/10.3384/ecp1511879

Gudmundsson, O., Schmidt, R.-R., Dyrelund, A., & Thorsen, J. E. (2022). Economic comparison of 4GDH and 5GDH systems – Using a case study. *Energy*, *238*, 121613. https://doi.org/10.1016/j.energy.2021.121613

Guelpa, E. (2020). Impact of network modelling in the analysis of district heating systems. *Energy*, *213*, 118393. https://doi.org/10.1016/j.energy.2020.118393

Guo, S., Ji, W., Wang, C., Song, T., & Wang, J. (2023). Hydraulic-thermal coupling dynamic models based on mechanism and data-driven methods of the heating networks in integrated energy systems. *Energy Conversion and Management*, *292*, 117353. https://doi.org/10.1016/j.enconman.2023.117353

Hua, P., Wang, H., Xie, Z., & Lahdelma, R. (2024). District heating load patterns and short-term forecasting for buildings and city level. *Energy*, *289*, 129866. https://doi.org/10.1016/j.energy.2023.129866

Klemm, C., Wiese, F., & Vennemann, P. (2023). Model-based run-time and memory reduction for a mixed-use multi-energy system model with high spatial resolution. *Applied Energy*, *334*, 120574. https://doi.org/10.1016/j.apenergy.2022.120574

Lund, H., Werner, S., Wiltshire, R., Svendsen, S., Thorsen, J. E., Hvelplund, F., & Mathiesen, B. V. (2014). 4th Generation District Heating (4GDH): Integrating smart thermal grids into future sustainable energy systems. *Energy*, *68*, 1–11. https://doi.org/10.1016/j.energy.2014.02.089

Moreno, D., Nielsen, S., Sorknæs, P., Lund, H., Thellufsen, J. Z., & Mathiesen, B. V. (2024). Exploring the location and use of baseload district heating supply. What can current heat sources tell us about future opportunities? *Energy*, *288*, 129642. https://doi.org/10.1016/j.energy.2023.129642

Oppelt, T., Urbaneck, T., Gross, U., & Platzer, B. (2016). Dynamic thermo-hydraulic model of district cooling networks. *Applied Thermal Engineering*, *102*, 336–345. https://doi.org/10.1016/j.applthermaleng.2016.03.168

Price, J. F. (2006). *Lagrangian and Eulerian Representations of Fluid Flow: Kinematics and the Equations of Motion*. MIT OpenCourseWare. https://ocw.mit.edu/courses/res-12-001-topics-in-fluid-dynamics-spring-

2022/pages/lagrangian-and-eulerian-representations-of-fluid-flow-kinematics-and-the-equations-of-motion/

Sartor, K., & Dewalef, P. (2017). Experimental validation of heat transport modelling in district heating networks. *Energy*, *137*, 961–968. https://doi.org/10.1016/j.energy.2017.02.161

Schweiger, G., Larsson, P.-O., Magnusson, F., Lauenburg, P., & Velut, S. (2017). District heating and cooling systems – Framework for Modelica-based simulation and dynamic optimization. *Energy*, *137*, 566–578. https://doi.org/10.1016/j.energy.2017.05.115

Steinegger, J., Wallner, S., Greiml, M., & Kienberger, T. (2023). A new quasi-dynamic load flow calculation for district heating networks. *Energy*, *266*, 126410. https://doi.org/10.1016/j.energy.2022.126410

Stevanovic, V. D., Prica, S., Maslovaric, B., Zivkovic, B., & Nikodijevic, S. (2007). Efficient numerical method for district heating system hydraulics. *Energy Conversion and Management*, *48*(5), 1536–1543. https://doi.org/10.1016/j.enconman.2006.11.018

van der Heijde, B., Aertgeerts, A., & Helsen, L. (2017). Modelling steady-state thermal behaviour of double thermal network pipes. *International Journal of Thermal Sciences*, *117*, 316–327. https://doi.org/10.1016/j.ijthermalsci.2017.03.026

van der Heijde, B., Fuchs, M., Ribas Tugores, C., Schweiger, G., Sartor, K., Basciotti, D., Müller, D., Nytsch-Geusen, C., Wetter, M., & Helsen, L. (2017). Dynamic equation-based thermo-hydraulic pipe model for district heating and cooling systems. *Energy Conversion and Management*, *151*, 158–169. https://doi.org/10.1016/j.enconman.2017.08.072

Volkova, A., Pakere, I., Murauskaite, L., Huang, P., Lepiksaar, K., & Zhang, X. (2022). 5th generation district heating and cooling (5GDHC) implementation potential in urban areas with existing district heating systems. *Energy Reports*, *8*, 10037–10047. https://doi.org/10.1016/j.egyr.2022.07.162

Wallentén, P. (1991). *Steady-state heat loss from insulated pipes*. Lund University.

Wang, H., & Meng, H. (2018). Improved thermal transient modeling with new 3-order numerical solution for a district heating network with consideration of the pipe wall's thermal inertia. *Energy*, *160*, 171–183. https://doi.org/10.1016/j.energy.2018.06.214

Wang, H., Meng, H., & Zhu, T. (2018). New model for onsite heat loss state estimation of general district heating network with hourly measurements. *Energy Conversion and Management*, *157*, 71–85. https://doi.org/10.1016/j.enconman.2017.11.062

Wang, Y., Wang, X., Zheng, L., Gao, X., Wang, Z., You, S., Zhang, H., & Wei, S. (2023). Thermo-hydraulic coupled analysis of long-distance district heating systems based on a fully-dynamic model. *Applied Thermal Engineering*, *222*, 119912. https://doi.org/10.1016/j.applthermaleng.2022.119912

Wang, Y., You, S., Zhang, H., Zheng, X., Zheng, W., Miao, Q., & Lu, G. (2017). Thermal transient prediction of district heating pipeline: Optimal selection of the time and spatial steps for fast and accurate calculation. *Applied Energy*, *206*, 900–910. https://doi.org/10.1016/j.apenergy.2017.08.061

Wu, L., Yin, X., Pan, L., & Liu, J. (2025). Smart energy management: Process structure-based hybrid neural networks for optimal scheduling and economic predictive control in integrated systems. *Applied Energy*, *380*, 124965. https://doi.org/10.1016/j.apenergy.2024.124965

Yıldırım, G. (2009). Computer-based analysis of explicit approximations to the implicit Colebrook–White equation in turbulent flow friction factor calculation. *Advances in Engineering Software*, *40*(11), 1183–1190. https://doi.org/10.1016/j.advengsoft.2009.04.004

Zheng, X., Shi, K., Wang, Y., You, S., Zhang, H., Zhu, C., Li, L., Wei, S., & Wang, N. (2020). Performance analysis of three iteration-free numerical methods for fast and accurate simulation of thermal dynamics in district heating pipeline. *Applied Thermal Engineering*, *178*, 115622. https://doi.org/10.1016/j.applthermaleng.2020.115622

Appendices

Appendix 1. Formulas of parameters in heat loss calculations

The parameters in Table 2 were calculated using the following equations.

$$T_s = \frac{T_h + T_c}{2} \tag{A.1}$$

$$T_a = \frac{T_h - T_c}{2} \tag{A.2}$$

$$\sigma = \frac{\lambda_i - \lambda_g}{\lambda_i + \lambda_g} \tag{A.3}$$

$$\gamma = \frac{2\left(1-\sigma^2\right)}{1-\sigma\left(\frac{r_o}{2H}\right)^2} \tag{A.4}$$

$$\beta = \frac{\lambda_g}{\lambda_i}\ln\left(\frac{r_o}{r_i}\right) \tag{A.5}$$

$$R = \frac{1}{2\pi\lambda_g}\left(\ln\left(\frac{2H}{r_o}\right)+\beta\right) \tag{A.6}$$

$$R_s = \frac{1}{2\pi\lambda_g}\left(\ln\left(\frac{2H}{r_o}\right)+\beta+\ln\left(\sqrt{1+\left(\frac{H}{D}\right)^2}\right)\right) \tag{A.7}$$

$$R_a = \frac{1}{2\pi\lambda_g}\left(\ln\left(\frac{2H}{r_o}\right)+\beta-\ln\left(\sqrt{1+\left(\frac{H}{D}\right)^2}\right)\right) \tag{A.8}$$

$$h_s^{-1} = \frac{2\lambda_i}{\lambda_g}\ln\left(\frac{2H}{r_o}\right) + \ln\left(\frac{r_o^2}{2Dr_i}\right) + \sigma\ln\left(\frac{r_o^4}{r_o^4 - D^4}\right) - \frac{\left(\frac{r_i}{2D} - \frac{2\sigma r_i D^3}{r_o^4 - D^4}\right)^2}{1 + \left(\frac{r_i}{2D}\right)^2 + \sigma\left(\frac{2r_i r_o^2 D}{r_o^4 - D^4}\right)^2} \quad (A.9)$$

$$h_a^{-1} = \ln\left(\frac{2D}{r_i}\right) + \sigma\ln\left(\frac{r_o^2 + D^2}{r_o^2 - D^2}\right) - \frac{\left(\frac{r_i}{2D} - \gamma\frac{Dr_i}{4H^2} + \frac{2\sigma r_i r_o^2 D}{r_o^4 - D^4}\right)^2}{1 - \left(\frac{r_i}{2D}\right)^2 - \gamma\frac{r_i}{2H} + 2\sigma r_i^2 r_o^2 \frac{r_o^4 + D^4}{\left(r_o^4 - D^4\right)^2}} - \gamma\left(\frac{D}{2H}\right)^2 \quad (A.10)$$

Here, T_h and T_c refer to the water temperatures of the hot and cold pipes, respectively. λ_i and λ_g are the heat conductivity of insulation and soil respectively. H is the buried depth from the pipe center to the ground surface. As shown in Figure 3, r_i and r_o are the outer radii of the pipe wall and the insulation, respectively. For twin pipes, D is the half-distance between the centers of the pipes.

Business, Economy

Art, Design, Architecture

Science, Technology

Crossover

Doctoral Theses

Aalto DT 75/2025

ISBN 978-952-64-2487-3
ISBN 978-952-64-2488-0 (pdf)

Aalto University
School of Science
Department of Mathematics
and System Analysis
aalto.fi